Accepted for publication in CMAME February 2010

A Natural–Norm Successive Constraint Method for Inf-Sup Lower Bounds

D.B.P. Huynh[*], D.J. Knezevic[†], Y. Chen[‡], J.S. Hesthaven[§], A.T. Patera[¶]

Abstract

We present a new approach for the construction of lower bounds for the inf-sup stability constants required in *a posteriori* error analysis of reduced basis approximations to affinely parametrized partial differential equations. We combine the "linearized" inf-sup statement of the natural–norm approach with the approximation procedure of the Successive Constraint Method (SCM): the former (natural–norm) provides an economical parameter expansion and local concavity in parameter — a small(er) optimization problem which enjoys intrinsic lower bound properties; the latter (SCM) provides a systematic optimization framework — a Linear Program (LP) relaxation which readily incorporates continuity and stability constraints. The natural–norm SCM requires a parameter domain decomposition: we propose a greedy algorithm for selection of the SCM control points as well as adaptive construction of the optimal subdomains. The efficacy of the natural–norm SCM is illustrated through numerical results for two types of non-coercive problems: the Helmholtz equation (for acoustics, elasticity, and electromagnetics), and the convection–diffusion equation.

Keywords: Reduced basis methods, natural–norm, Successive Constraint Method (SCM), inf-sup constant, lower bound, Helmholtz, acoustics, elasticity, Maxwell, convection–diffusion.

1 Introduction

The certified reduced basis method is well developed for both coercive and non-coercive elliptic affinely parametrized partial differential equations [11, 15, 17].

[*]Mechanical Engineering Department, National University of Singapore, baophuonghk@gmail.com

[†]Mechanical Engineering Department, Massachusetts Institute of Technology, dknez@mit.edu

[‡]Division of Applied Mathematics, Brown University, yanlai_chen@brown.edu

[§]Division of Applied Mathematics, Brown University, jan.hesthaven@brown.edu

[¶]Corresponding author; Mechanical Engineering Department, Massachusetts Institute of Technology, patera@mit.edu

The reduced basis approximation of dimension N is built upon (and the reduced basis error is measured with respect to) an underlying truth discretization of dimension $\mathcal{N}$ which we wish to "accelerate." The essential acceleration ingredients are Galerkin projection onto a low dimensional space associated with an optimally sampled smooth parametric manifold [1, 5, 12, 14] — rapid convergence; rigorous *a posteriori* error bounds for the field variable and associated functional outputs of interest — reliability and control; and Offline–Online computational decomposition strategies — rapid response in the real–time and many-query contexts. In the Online stage, given a new parameter value, we rapidly calculate the reduced basis (output) approximation and associated reduced basis error bound: the operation count is independent of $\mathcal{N}$ and depends only on $N \ll \mathcal{N}$ and Q; here Q is the number of terms in the affine parameter expansion of the operator.

The *a posteriori* error bound requires an estimate for the stability factor — coercivity constant or inf-sup constant — associated with the partial differential operator. (Although we retain the usual terminology of "constant," in actual fact the parametric dependence of these stability factors is crucial and the focus of this paper.) This stability factor estimate must satisfy several requirements:

(i) it must be a provably strict lower bound for the true stability factor (associated with the truth discretization);

(ii) it must be a reasonably accurate approximation — O(1) relative error — of the true stability factor;

(iii) it must admit an Offline–Online computational treatment, based on the affine parametrization of the partial differential equation, for which the Online effort is independent of $\mathcal{N}$.

Although it is simple to develop effective *upper* bounds for stability factors [8, 9, 13], it is much more difficult to efficiently provide rigorous *lower bounds* for stability factors.

There are several approaches to stability factor lower bounds within the Offline–Online reduced basis context; each approach may be characterized by the inf-sup formulation and the lower bound procedure. A "natural–norm" method is proposed in [4, 18]: the linearized–in–parameter inf-sup formulation has several desirable approximation properties — a Q–term affine parameter expansion, and first order (in parameter) concavity; however, the lower bound procedure is rather crude — a framework which incorporates only continuity information. A Successive Constraint Method (SCM) is proposed in [2, 7, 17]: the lower bound procedure is rather efficient — a framework which incorporates both continuity *and* stability information; however, the classical inf-sup formulation (in which the operator is effectively squared, albeit in the proper norm) has several undesirable attributes — a Q^2–term affine parameter expansion, and loss of (even local) concavity. Clearly the two approaches are complementary.

In this paper we combine the "linearized" inf-sup statement introduced in [18] with the SCM lower bound procedure proposed in [2, 7, 17]. The former

(natural–norm) provides a Q–term affine parameter expansion and local concavity in parameter: a small(er) optimization problem which enjoys intrinsic lower bound properties. The latter (SCM) provides a systematic optimization framework: a Linear Program (LP) relaxation which readily incorporates effective stability constraints. From a theoretical perspective, the combined "natural–norm SCM" can be placed on a firm basis in particular for the important class of Helmholtz problems. And from the computational perspective, the natural–norm SCM performs very well in particular in the Offline stage: the natural–norm SCM is typically an order of magnitude less costly than either the natural–norm or "classical" SCM approaches alone. We present numerical results to justify these claims.

In Section 2 we present the general (weak) formulation for second–order non-coercive elliptic partial differential equations. In Section 3 we introduce the new "natural–norm SCM": a local inf-sup approximation, a greedy sampling strategy for construction of a global inf-sup approximation, and finally the incorporation of the global inf-sup bound into reduced basis *a posteriori* error estimators as regards both the Offline and Online stages. In Section 4 we apply the procedure to several examples of the Helmholtz equation in the context of acoustics, elasticity, and electromagnetics. Section 5 apples the procedure to an example of the convection–diffusion equation (relevant to Fokker–Planck treatment of polymeric fluids [10]) while Section 6 contains a few concluding remarks.

In what follows, we denote the classical SCM method [2, 7, 17] as "classical SCM^2" or simply SCM^2 in order to avoid confusion with the new "natural–norm SCM" method: here the (squared) superscript suggests the undesired Q^2–term affine parameter expansion in the "classical SCM^2" method.

2 Formulation

Let us introduce the (bounded) physical domain $\Omega \subset \mathbb{R}^2$ with boundary $\partial\Omega$; we shall denote a point in Ω by $x = (x_1, x_2)$. We also introduce our closed parameter domain $\mathcal{D} \in \mathbb{R}^P$, a point in which we shall denote $\mu = (\mu_1, \ldots, \mu_P)$. Let us then define the Hilbert space X equipped with inner product $(\cdot,\cdot)_X$ and induced norm $\|\cdot\|_X$. Here $(H_0^1(\Omega))^{\mathcal{V}} \subset X \subset (H^1(\Omega))^{\mathcal{V}}$ ($\mathcal{V} = 1$ for a scalar field and $\mathcal{V} > 1$ for a vector field), where $H^1(\Omega) = \{v \in L^2(\Omega), \nabla v \in (L^2(\Omega))^2\}$, $L^2(\Omega)$ is the space of square integrable functions over Ω, and $H_0^1(\Omega) = \{v \in H^1(\Omega) |\ v|_{\partial\Omega} = 0\}$ [16]; for inner product and norm we consider

$$(w, v)_X = \int_\Omega \nabla w \cdot \nabla v + \tau \int_\Omega wv, \quad \|w\|_X = \{(w, w)_X\}^{1/2}$$

or suitable (equivalent) variants. The (parameter independent) τ is chosen as

$$\tau = \inf_{w \in X} \frac{\int_\Omega \nabla w \cdot \nabla w}{\int_\Omega ww} \ ;$$

this choice provides rapid convergence of the Lanczos procedure for the discrete inf-sup parameter [17]. In the case of the two-dimensional Maxwell example of Section 4.5 our space must be modified: Let

$$X = H_0(\text{curl};\Omega) = \left\{ v \in \left(L^2(\Omega)\right)^2 \,|\, (\nabla \times v) \cdot \widehat{z} \in L^2(\Omega),\ \widehat{n} \times v = 0 \text{ on } \partial\Omega \right\}$$

where, in two-dimensions, $\nabla \times v = (\frac{\partial}{\partial x}, \frac{\partial}{\partial y}, 0) \times (v_1, v_2, 0)$, $\widehat{z}$ is the unit vector along the x_3-axis and $\widehat{n} = (n_1, n_2, 0)$ is the unit outward normal to $\partial\Omega$; X is equipped with the following inner product and induced norm

$$(w, v)_{H(\text{curl})} = \int_\Omega \nabla \times w \cdot \nabla \times v + \int_\Omega wv, \quad \|w\|_{H(\text{curl})} = \left\{(w, w)_{H(\text{curl})}\right\}^{1/2}.$$

Note that we include the boundary conditions in X for the Maxwell case since we consider only a single example of this type in Section 4; this is, however, not an essential restriction.

Let us next introduce a parametrized bilinear form $a(\cdot, \cdot; \mu)$: $X \times X \to \mathbb{R}$ and suppose it is inf-sup stable and continuous over X: $\beta(\mu) > 0$ and $\gamma(\mu)$ is finite $\forall \mu \in \mathcal{D}$, where

$$\beta(\mu) = \inf_{w \in X} \sup_{v \in X} \frac{a(w, v; \mu)}{\|w\|_X \, \|v\|_X},$$

and

$$\gamma(\mu) = \sup_{w \in X} \sup_{v \in X} \frac{a(w, v; \mu)}{\|w\|_X \, \|v\|_X}.$$

Further assume that a is "affine" in the parameter such that

$$a(w, v; \mu) = \sum_{q=1}^{Q} \Theta_q(\mu) a_q(w, v), \tag{1}$$

where $\Theta_q(\cdot)$: $\mathcal{D} \to \mathbb{R}$ and $a_q(\cdot, \cdot)$: $X \times X \to \mathbb{R}$ are *parameter-dependent* functions and *parameter-independent* bilinear forms, respectively, for $1 \le q \le Q$. Finally, we introduce two linear bounded functionals $f : X \to \mathbb{R}$ and $\ell : X \to \mathbb{R}$. We may then introduce our (well–posed) continuous problem: Given $\mu \in \mathcal{D}$, find $u(\mu) \in X$ such that

$$a(u(\mu), v; \mu) = f(v), \forall v \in X,$$

and then evaluate the scalar output of interest as $s(\mu) = \ell(u(\mu))$. (In practice, f and ℓ may also depend (affinely) on the parameter.)

We comment briefly on the treatment of geometry. The problem of interest is first posed on a (potentially) parameter–dependent "original" domain $\Omega^o(\mu)$. We then map $\Omega^o(\mu)$ to a reference domain $\Omega = \Omega(\mu_{\text{ref}})$ by application of piecewise affine transformations over a coarse triangulation.[1] The geometric factors associated with the mapping are then reflected in the coefficient functions

[1] We restrict attention in this paper to polygonal domains $\Omega(\mu)$ for which such a coarse triangulation and associated affine transformations can always be found; more general curved boundaries can in fact also be treated in many instances [17].

$\Theta_q, 1 \le q \le Q$. For some simple problems, such as the Helmholtz "microphone" problem of Section 4.2, the necessary mapping and identification of the affine form can be performed "by hand"; in other cases, such as the Helmholtz examples in Sections 4.3–4.4, automatic procedures [6] should be applied both for convenience (to avoid laborious "by hand" algebraic manipulations) and efficiency (smaller Q implies more efficient inf-sup lower bounds).

Consider next a truth finite element approximation space $X^{\mathcal{N}} \subset X$. Suppose that $\mathcal{N}$ is chosen sufficiently large that a remains inf-sup stable (and continuous) over $X^{\mathcal{N}}$: $\beta^{\mathcal{N}}(\mu) > 0$ and $\gamma^{\mathcal{N}}(\mu)$ is finite $\forall \mu \in \mathcal{D}$, where

$$\beta^{\mathcal{N}}(\mu) = \inf_{w \in X^{\mathcal{N}}} \sup_{v \in X^{\mathcal{N}}} \frac{a(w, v; \mu)}{\|w\|_X \, \|v\|_X},$$

and

$$\gamma^{\mathcal{N}}(\mu) = \sup_{w \in X^{\mathcal{N}}} \sup_{v \in X^{\mathcal{N}}} \frac{a(w, v; \mu)}{\|w\|_X \, \|v\|_X}.$$

We now introduce our truth discretization: Given $\mu \in \mathcal{D}$, find $u^{\mathcal{N}}(\mu) \in X^{\mathcal{N}}$ such that

$$a(u^{\mathcal{N}}(\mu), v; \mu) = f(v), \forall v \in X^{\mathcal{N}},$$

and then evaluate the output as $s^{\mathcal{N}}(\mu) = \ell(u^{\mathcal{N}}(\mu))$. In what follows we build our reduced basis approximation upon, and measure the error in our reduced basis approximation with respect to, the truth discretization: for clarity of exposition we shall suppress the $\mathcal{N}$ except as needed (for example) to demonstrate uniformity as $\mathcal{N} \to \infty$.

Introduce the supremizing operator $T^\mu : X \to X$ such that $(T^\mu w, v)_X = a(w, v; \mu), \forall v \in X$. It is readily demonstrated that

$$T^\mu w = \arg \sup_{v \in X} \frac{a(w, v; \mu)}{\|v\|_X},$$

and that furthermore

$$\beta(\mu) = \inf_{w \in X} \frac{\|T^\mu w\|_X}{\|w\|_X}.$$

Also note that T^μ may be expressed as

$$T^\mu w = \sum_{q=1}^{Q} \Theta_q(\mu) T_q w$$

where $(T_q w, v)_X = a_q(w, v), \forall v \in X$, $1 \le q \le Q$, due to the affine assumption.

3 Natural–Norm SCM Lower Bound

3.1 Local Approximation

We now introduce a subdomain of $\mathcal{D}$, $\mathcal{D}_{\bar{\mu}}$, associated (in a way we shall subsequently make precise) to a particular parameter point $\bar{\mu}$ in $\mathcal{D}$. In this subsection

we develop a local lower bound "building block"; in the next section we exploit these building blocks to construct a global lower bound for the inf-sup constant over $\mathcal{D}$.

Let us first define an inf-sup constant measured relative to a natural–norm [18]: given a $\mu \in \mathcal{D}_{\bar{\mu}}$,

$$\beta_{\bar{\mu}}(\mu) = \inf_{w \in X} \sup_{v \in X} \frac{a(w, v; \mu)}{\|T^{\bar{\mu}} w\|_X \|v\|_X};$$

of course $\|T^{\bar{\mu}} \cdot\|_X$ is a well-defined norm and in fact equivalent to $\|\cdot\|_X$ since $\beta(\mu)$ is positive for all $\mu \in \mathcal{D}$. Next introduce [18] a lower bound for $\beta_{\bar{\mu}}(\mu)$,

$$\bar{\beta}_{\bar{\mu}}(\mu) = \inf_{w \in X} \frac{a(w, T^{\bar{\mu}} w; \mu)}{\|T^{\bar{\mu}} w\|_X^2}.$$

It is clear that $\bar{\beta}_{\bar{\mu}}(\mu) \leq \beta_{\bar{\mu}}(\mu)$ and that furthermore $\bar{\beta}_{\bar{\mu}}(\mu)$ will be a good approximation to $\beta_{\bar{\mu}}(\mu)$ for μ near $\bar{\mu}$ [18]. (In fact, it is readily demonstrated that $\beta(\bar{\mu})\bar{\beta}_{\bar{\mu}}(\mu) \leq \beta(\mu)$, and hence we can translate the lower bound for $\bar{\beta}_{\bar{\mu}}(\mu)$ into a lower bound for $\beta(\mu)$ — our ultimate goal. We reserve this finishing touch for Proposition 3 of Section 3.2; our focus here is the lower bound for $\bar{\beta}_{\bar{\mu}}(\mu)$ and hence $\beta_{\bar{\mu}}(\mu)$.)[2]

Next we apply the Successive Constraint Method (SCM) to construct lower and upper bounds for $\bar{\beta}_{\bar{\mu}}(\mu)$. First note that

$$\bar{\beta}_{\bar{\mu}}(\mu) = \inf_{y \in \mathcal{Y}_{\bar{\mu}}} \mathcal{J}(y; \mu),$$

where

$$\mathcal{J}(y; \mu) = \sum_{q=1}^{Q} \Theta_q(\mu) y_q$$

and

$$\mathcal{Y}_{\bar{\mu}} = \{y \in \mathbb{R}^Q \mid \exists\, w_y \in X \text{ s.t. } y_q = \frac{a_q(w_y, T^{\bar{\mu}} w_y)}{\|T^{\bar{\mu}} w_y\|_X^2}, \quad 1 \leq q \leq Q\}.$$

Let us now proceed to formulate a lower bound and subsequently an upper bound.

First introduce the box

$$\mathcal{B}_{\bar{\mu}} = \prod_{q=1}^{Q} \left[-\frac{\gamma_q}{\beta(\bar{\mu})}, \frac{\gamma_q}{\beta(\bar{\mu})} \right],$$

where

$$\gamma_q = \sup_{w \in X} \frac{\|T_q w\|_X}{\|w\|_X}, \quad 1 \leq q \leq Q;$$

[2]Note that we express the bilinear form $a(w, T^{\bar{\mu}} v; \mu)$ associated with $\bar{\beta}_{\bar{\mu}}(\mu)$ in the symmetrized form $\frac{1}{2} a(w, T^{\bar{\mu}} v; \mu) + \frac{1}{2} a(v, T^{\bar{\mu}} w; \mu)$ to facilitate numerical evaluation.

note that the γ_q are independent of $\bar{\mu}$. Next introduce the SCM sample

$$\mathcal{C}_{\bar{\mu}} = \{\hat{\mu}_{\bar{\mu}}^1, \ldots, \hat{\mu}_{\bar{\mu}}^{J_{\bar{\mu}}}\}.$$

We can now define

$$\mathcal{Y}_{\bar{\mu}}^{\mathrm{LB}}(\mathcal{C}_{\bar{\mu}}) = \{y \in \mathcal{B}_{\bar{\mu}} \mid \sum_{q=1}^{Q} \Theta_q(\mu') y_q \geq \bar{\beta}_{\bar{\mu}}(\mu'), \forall \mu' \in \mathcal{C}_{\bar{\mu}}\},$$

and then

$$\bar{\beta}_{\bar{\mu}}^{\mathrm{LB}}(\mu; \mathcal{C}_{\bar{\mu}}) = \inf_{y \in \mathcal{Y}_{\bar{\mu}}^{\mathrm{LB}}(\mathcal{C}_{\bar{\mu}})} \mathcal{J}(y; \mu), \forall \mu \in \mathcal{D}_{\bar{\mu}}. \tag{2}$$

We will shortly provide two propositions for the construction (2).

Let us next develop the upper bound. Our primary interest is in the lower bound — as required for rigor in our reduced basis *a posteriori* error estimator. However, the upper bound serves an important role in the greedy algorithm by which we construct an effective lower bound. We first introduce the set

$$\mathcal{Y}_{\bar{\mu}}^{\mathrm{UB}}(\mathcal{C}_{\bar{\mu}}) = \{y_{\bar{\mu}}^*(\hat{\mu}_{\bar{\mu}}^j), 1 \leq j \leq J_{\bar{\mu}}\}$$

where

$$y_{\bar{\mu}}^*(\mu) = \arg\min_{y \in \mathcal{Y}_{\bar{\mu}}} \mathcal{J}(y; \mu);$$

we then define

$$\bar{\beta}_{\bar{\mu}}^{\mathrm{UB}}(\mu; \mathcal{C}_{\bar{\mu}}) = \inf_{y \in \mathcal{Y}_{\bar{\mu}}^{\mathrm{UB}}(\mathcal{C}_{\bar{\mu}})} \mathcal{J}(y; \mu), \quad \forall \mu \in \mathcal{D}_{\bar{\mu}}. \tag{3}$$

It is simple to demonstrate that $\mathcal{Y}_{\bar{\mu}}^{\mathrm{UB}}(\mathcal{C}_{\bar{\mu}}) \subset \mathcal{Y}_{\bar{\mu}} \subset \mathcal{Y}_{\bar{\mu}}^{\mathrm{LB}}(\mathcal{C}_{\bar{\mu}})$ and hence

Proposition 1 *The approximations* (2) *and* (3) *satisfy*

$$\bar{\beta}_{\bar{\mu}}^{\mathrm{UB}}(\mu; \mathcal{C}_{\bar{\mu}}) \geq \bar{\beta}_{\bar{\mu}}(\mu) \geq \bar{\beta}_{\bar{\mu}}^{\mathrm{LB}}(\mu; \mathcal{C}_{\bar{\mu}})$$

for all μ *in* $\mathcal{D}_{\bar{\mu}}$.

Proof. The proof is analogous to the proof of Proposition 1 in [7]. As in [7], it is clear that $\mathcal{Y}_{\bar{\mu}}^{\mathrm{UB}}(\mathcal{C}_{\bar{\mu}}) \subset \mathcal{Y}_{\bar{\mu}}$, and hence we focus on the lower bound result here. For any $w \in X^{\mathcal{N}}$ we have $a_q(w, T^{\bar{\mu}} w) = (T_q w, T^{\bar{\mu}} w)_X$, and furthermore for any $y \in \mathcal{Y}_{\bar{\mu}}$ there is a $w_y \in X^{\mathcal{N}}$ satisfying $y_q = \dfrac{a_q(w_y, T^{\bar{\mu}} w_y)}{\|T^{\bar{\mu}} w_y\|_X^2}$, $1 \leq q \leq Q$. Therefore, for any $y \in \mathcal{Y}_{\bar{\mu}}$

$$|y_q| = \frac{|(T_q w_y, T^{\bar{\mu}} w_y)_X|}{\|T^{\bar{\mu}} w_y\|_X^2} \leq \frac{\|T_q w_y\|_X}{\|T^{\bar{\mu}} w_y\|_X} = \frac{\|T_q w_y\|_X}{\|w_y\|_X} \frac{\|w_y\|_X}{\|T^{\bar{\mu}} w_y\|_X} \leq \frac{\gamma_q}{\beta(\bar{\mu})};$$

also,

$$\sum_{q=1}^{Q}\Theta_q(\mu')y_q = \sum_{q=1}^{Q}\Theta_q(\mu')\frac{a_q(w_y,T^{\bar{\mu}}w_y)}{\|T^{\bar{\mu}}w_y\|_X^2}$$
$$\geq \inf_{w\in X^{\mathcal{N}}}\sum_{q=1}^{Q}\Theta_q(\mu')\frac{a_q(w,T^{\bar{\mu}}w)}{\|T^{\bar{\mu}}w\|_X^2} = \bar{\beta}_{\bar{\mu}}(\mu'),$$

for all $\mu' \in \mathcal{C}_{\bar{\mu}}$. Hence $\mathcal{Y}_{\bar{\mu}} \subset \mathcal{Y}_{\bar{\mu}}^{\rm LB}(\mathcal{C}_{\bar{\mu}})$, from which $\bar{\beta}_{\bar{\mu}}(\mu) \geq \bar{\beta}_{\bar{\mu}}^{\rm LB}(\mu;\mathcal{C}_{\bar{\mu}})$ follows easily. □

We can further demonstrate for the more important lower bound

Proposition 2 *Under the assumption that the $\Theta_q(\mu), 1 \leq q \leq Q$, are affine functions of μ,*

$$\bar{\beta}_{\bar{\mu}}^{\rm LB}(\mu;\mathcal{C}_{\bar{\mu}}) \geq \sup_{\sigma\in\mathcal{S}_{J_{\bar{\mu}}}(\mu;\mathcal{C}_{\bar{\mu}})}\sum_{j=1}^{J_{\bar{\mu}}}\sigma_j\bar{\beta}_{\bar{\mu}}(\hat{\mu}_{\bar{\mu}}^j)$$

for all μ in $\mathcal{D}_{\bar{\mu}}$. Here $\mathcal{S}_{J_{\bar{\mu}}}(\mu;\mathcal{C}_{\bar{\mu}})$ is the set of $J_{\bar{\mu}}$–tuples σ such that

$$\sum_{j=1}^{J_{\bar{\mu}}}\sigma_j = 1, \qquad \sum_{j=1}^{J_{\bar{\mu}}}\sigma_j\hat{\mu}_{\bar{\mu}}^j = \mu$$

and $0 \leq \sigma_j \leq 1, 1 \leq j \leq J_{\bar{\mu}}$.

Proof. Let σ be an arbitrary element of $\mathcal{S}_{J_{\bar{\mu}}}(\mu;\mathcal{C}_{\bar{\mu}})$. Then,

$$\bar{\beta}_{\bar{\mu}}^{\rm LB}(\mu;\mathcal{C}_{\bar{\mu}}) = \inf_{y\in\mathcal{Y}_{\bar{\mu}}^{\rm LB}(\mathcal{C}_{\bar{\mu}})}\mathcal{J}(y;\mu) = \inf_{y\in\mathcal{Y}_{\bar{\mu}}^{\rm LB}(\mathcal{C}_{\bar{\mu}})}\sum_{q=1}^{Q}\Theta_q(\sum_{j=1}^{J_{\bar{\mu}}}\sigma_j\hat{\mu}_{\bar{\mu}}^j)\,y_q$$
$$= \inf_{y\in\mathcal{Y}_{\bar{\mu}}^{\rm LB}(\mathcal{C}_{\bar{\mu}})}\sum_{j=1}^{J_{\bar{\mu}}}\sigma_j\sum_{q=1}^{Q}\Theta_q(\hat{\mu}_{\bar{\mu}}^j)\,y_q \geq \sum_{j=1}^{J_{\bar{\mu}}}\sigma_j\inf_{y\in\mathcal{Y}_{\bar{\mu}}^{\rm LB}(\mathcal{C}_{\bar{\mu}})}\sum_{q=1}^{Q}\Theta_q(\hat{\mu}_{\bar{\mu}}^j)\,y_q$$
$$= \sum_{j=1}^{J_{\bar{\mu}}}\sigma_j\bar{\beta}_{\bar{\mu}}(\hat{\mu}_{\bar{\mu}}^j).$$

Since the result is valid for any $\sigma \in \mathcal{S}_{J_{\bar{\mu}}}(\mu;\mathcal{C}_{\bar{\mu}})$ we may then take the sup — our bound will do at least as well as the best combination. □

We note that when saying that our weak form is "affine" in the parameter, (1), we mean more precisely that the weak form is affine in *functions* of the parameter — the $\Theta_q(\mu), 1 \leq q \leq Q$. In contrast, when we say (additionally) that our coefficient functions $\Theta_q(\mu), 1 \leq q \leq Q$, are affine functions of μ, we refer

to the standard definition. The assumption on the weak form, (1), is crucial; the assumption on the coefficient functions serves primarily for interpretation and theoretical motivation.

Two cautionary notes. First, in Proposition 1, the lower bound will only be useful if $\bar{\beta}_{\bar{\mu}}(\mu) > 0$ over $\mathcal{D}_{\bar{\mu}}$: in general the latter is not a consequence of our (necessary) hypothesis $\beta(\mu) > 0, \forall \mu \in \mathcal{D}_{\bar{\mu}}$; we must thus adaptively divide the actual parameter domain of interest $\mathcal{D}$ into subdomains or "elements" $\mathcal{D}_{\bar{\mu}}$ such that positivity is ensured. Second, in Proposition 2, most problems, in particular with any geometric parameter variation, will yield functions $\Theta_q(\mu), 1 \le q \le Q$, that are *not* affine in μ; there will thus be $\mathrm{O}(|\mu - \bar{\mu}|^2)$ corrections to our result (2) — controlled by the box constraints $\mathcal{B}_{\bar{\mu}}$ — which will further implicitly restrict the extent of $\mathcal{D}_{\bar{\mu}}$.

3.2 Global Approximation: Greedy Sampling Procedure

We construct our domain decomposition $\mathcal{D}_{\bar{\mu}^k}, 1 \le k \le K$, by a greedy approach similar to the greedy approach applied within earlier SCM proposals. For the purposes of this section, let us extend our lower and upper bounds of (2) and (3) to all $\mu \in \mathcal{D}$: for a given $\bar{\mu} \in \mathcal{D}$ and a finite sample $\mathcal{E} \subset \mathcal{D}$ we define

$$g_{\bar{\mu}}^{\mathrm{LB}}(\mu; \mathcal{E}) = \inf_{y \in \mathcal{Y}_{\bar{\mu}}^{\mathrm{LB}}(\mathcal{E})} \mathcal{J}(y; \mu), \forall \mu \in \mathcal{D},$$

and

$$g_{\bar{\mu}}^{\mathrm{UB}}(\mu; \mathcal{E}) = \inf_{y \in \mathcal{Y}_{\bar{\mu}}^{\mathrm{UB}}(\mathcal{E})} \mathcal{J}(y; \mu), \forall \mu \in \mathcal{D}.$$

Now introduce an "SCM quality control" indicator

$$\epsilon_{\bar{\mu}}(\mu; \mathcal{E}) \equiv \frac{g_{\bar{\mu}}^{\mathrm{UB}}(\mu; \mathcal{E}) - g_{\bar{\mu}}^{\mathrm{LB}}(\mu; \mathcal{E})}{g_{\bar{\mu}}^{\mathrm{UB}}(\mu; \mathcal{E})} \ \forall \mu \in \mathcal{D}.$$

an SCM tolerance $\epsilon_{\bar{\beta}} \in (0, 1)$, and an inf-sup tolerance — a non-negative function $\varphi(\mu, \bar{\mu})$. Most simply we may set this latter function to zero, however other choices may also be of interest; we discuss this further, in the next subsection, in the reduced basis error estimation context in which our inf-sup lower bound shall ultimately serve. Finally, we require a very rich train sample $\Xi \in \mathcal{D}$.

Let us now define the greedy algorithm in Algorithm 1. Note that the set of points $\mathcal{R}$ play the role of temporary subdomains during the greedy construction — note also that we define the "size" of $\mathcal{R}$ to be the cardinality, $|\mathcal{R}|$. Observe that in Step 3 of the algorithm there is only one condition under which we declare the current subdomain/approximation complete (and move to the next subdomain): the trial sample offers no improvement in the positivity coverage *and* the trial sample is not required to satisfy our $\epsilon_{\bar{\beta}}$ SCM quality criterion; in this case we discard the trial point μ^* and proceed to identify the next subdomain. The "output" from the greedy procedure is the set of points $S = \{\bar{\mu}^1, \ldots, \bar{\mu}^K\}$ and associated SCM sample sets $\mathcal{C}_{\bar{\mu}^k}, 1 \le k \le K$.

Algorithm 1 Natural–Norm SCM Greedy Algorithm

1. Set $S = \{\bar{\mu}^1\}$, $\mathcal{C}_{\bar{\mu}^1} = \{\bar{\mu}^1\}$, $J_{\bar{\mu}^1} = 1$, $k = 1$; here $\bar{\mu}^1$ is an arbitrary point in Ξ;

2. Find

$$\mu^* = \arg\max_{\mu\in\Xi} \epsilon_{\bar{\mu}^k}(\mu; \mathcal{C}_{\bar{\mu}^k})$$

and append μ^* to $\mathcal{C}_{\bar{\mu}^k}$ to form a "trial" sample $\mathcal{C}^*_{\bar{\mu}^k}$;
if $J_{\bar{\mu}^k} = 1$ **then**
  Construct $\mathcal{R}_{\bar{\mu}^k}$ to be the set of all points $\mu \in \Xi$ such that $g^{\rm LB}_{\bar{\mu}^k}(\mu; \mathcal{C}_{\bar{\mu}^k}) > \varphi(\mu, \bar{\mu}^k)$;
end if

3. Construct $\mathcal{R}^*_{\bar{\mu}^k}$ to be the set of all points $\mu \in \Xi$ such that $g^{\rm LB}_{\bar{\mu}^k}(\mu; \mathcal{C}^*_{\bar{\mu}^k}) > \varphi(\mu, \bar{\mu}^k)$;
if $\mathcal{R}^*_{\bar{\mu}^k} \backslash \mathcal{R}_{\bar{\mu}^k} = \{\}$ **and** $\epsilon_{\bar{\mu}^k}(\mu; \mathcal{C}_{\bar{\mu}^k}) < \epsilon_{\bar{\beta}}, \forall \mu \in \Xi$, **then**
  goto 4;
else
  Set $\mathcal{C}_{\bar{\mu}^k} = \mathcal{C}^*_{\bar{\mu}^k}$, $\mathcal{R}_{\bar{\mu}^k} = \mathcal{R}^*_{\bar{\mu}^k}$, $J_{\bar{\mu}^k} \leftarrow J_{\bar{\mu}^k} + 1$, and **goto** 2;
end if

4. Update (prune) $\Xi \leftarrow \Xi \backslash \mathcal{R}_{\bar{\mu}^k}$;
if $\Xi = \{\}$, **then**
  Set $K = k$ and **terminate**;
else
  Find

$$\bar{\mu}^{k+1} = \arg\min_{\mu\in\Xi} g^{\rm LB}_{\bar{\mu}^k}(\mu; \mathcal{C}_{\bar{\mu}^k}),$$

  append $\bar{\mu}^{k+1}$ to S, set $k \leftarrow k + 1$, initialize $\mathcal{C}_{\bar{\mu}^k} = \{\bar{\mu}^k\}$, $J_{\bar{\mu}^k} = 1$, and **goto** 2;
end if

The improvement for a particular subdomain and identification of a new subdomain are based on different criteria. For the former $\epsilon_{\bar{\mu}^k}(\mu; \mathcal{C}_{\bar{\mu}^k})$ is very effective: the arg max will *avoid* μ for which the upper bound is negative and hence likely to lie outside the domain of relevance of $T^{\bar{\mu}^k}$, yet *favor* μ for which the current approximation is poor and hence (likely) to lie at the extremes of the domain of relevance of $T^{\bar{\mu}^k}$ — thus promoting optimal coverage. In contrast, for the latter $g^{\rm LB}_{\bar{\mu}^k}$ is very effective: the arg min will look for the most negative value of the lower bound — thus leaving the domain of relevance of $T^{\bar{\mu}^k}$. In the Helmholtz examples, the subdomains will roughly correspond to regions between resonances: we first outline a particular resonance and we then "jump" to the next resonance.

Let us now define our global lower bound for $\bar{\beta}(\mu)$ as

$$\beta^{\rm LB}(\mu) = \beta(\bar{\mu}^{k^*}) g^{\rm LB}_{\bar{\mu}^{k^*}}(\mu; \mathcal{C}_{\bar{\mu}^{k^*}}) \tag{4}$$

where

$$k^*(\mu) = \arg \max_{k \in \{1 \ldots K\}} \beta(\bar{\mu}^k) g^{\rm LB}_{\bar{\mu}^k}(\mu; \mathcal{C}_{\bar{\mu}^k}). \tag{5}$$

Note that (5) also implicitly defines our subdomains for $1 \le k \le K$:

$$\mathcal{D}_{\bar{\mu}^k} = \left\{ \mu \in \mathcal{D} \mid \beta(\bar{\mu}^k) g^{\rm LB}_{\bar{\mu}^k}(\mu; \mathcal{C}_{\bar{\mu}^k}) \ge \beta(\bar{\mu}^{k'}) g^{\rm LB}_{\bar{\mu}^{k'}}(\mu; \mathcal{C}_{\bar{\mu}^{k'}}),\ \forall k' \in \{1, \ldots, K\} \right\}.$$

Based on this, we have

Proposition 3 *The approximation* (4) *satisfies*

$$\beta^{\rm LB}(\mu) \le \beta(\mu)$$

for all μ *in* $\mathcal{D}$.

Proof. For any $\mu \in \mathcal{D}$ and any $\bar{\mu}^k \in S$, we have

$$\begin{aligned}
\beta(\mu) &= \inf_{w \in X^{\mathcal{N}}} \sup_{v \in X^{\mathcal{N}}} \frac{a(w,v;\mu)}{\|w\|_X \|v\|_X} = \inf_{w \in X^{\mathcal{N}}} \sup_{v \in X^{\mathcal{N}}} \frac{a(w,v;\mu)}{\|T^{\bar{\mu}^k} w\|_X \|v\|_X} \frac{\|T^{\bar{\mu}^k} w\|_X}{\|w\|_X} \\
&\ge \inf_{w \in X^{\mathcal{N}}} \sup_{v \in X^{\mathcal{N}}} \frac{a(w,v;\mu)}{\|T^{\bar{\mu}^k} w\|_X \|v\|_X} \inf_{w \in X^{\mathcal{N}}} \frac{\|T^{\bar{\mu}^k} w\|_X}{\|w\|_X} \\
&= \beta_{\bar{\mu}^k}(\mu)\, \beta(\bar{\mu}^k) \ge \bar{\beta}_{\bar{\mu}^k}(\mu)\, \beta(\bar{\mu}^k) \ge g^{\rm LB}_{\bar{\mu}^k}(\mu; \mathcal{C}_{\bar{\mu}^k}) \beta(\bar{\mu}^k),
\end{aligned}$$

where the final inequality follows from Proposition 1. This clearly holds for $k = k^*(\mu)$, and hence the proof is complete. □

It is worth making two comments related to the interpolation properties of the method. Firstly, since $\beta^{\rm LB}(\bar{\mu}) = \beta(\bar{\mu})$, the method interpolates β at each $\bar{\mu} \in S$. Secondly, from the concavity argument in Proposition 2, the extreme points of the $\mathcal{D}_{\bar{\mu}}$ (where β will tend to be small) will be well approximated — which is important for positivity.

3.3 Reduced Basis: *A Posteriori* Error Estimators

Let us first describe how the inf-sup lower bound will serve within the reduced basis context and then summarize the Offline and Online stages of the process. We now suppose that we are given a reduced basis field approximation $u_N(\mu)$ and output approximation $s_N(\mu) = \ell(u_N)$. We further introduce the reduced basis residual,

$$r(v;\mu) \equiv f(v) - a(u_N, v; \mu), \forall v \in X.$$

The reduced basis output error (relative to the truth discretization) then satisfies

Proposition 4 *For any $\mu \in \Xi$ and more generally any μ in $\mathcal{D}$ such that the lower bound* (4) *is positive, the reduced basis output error satisfies*

$$|s^{\mathcal{N}}(\mu) - s_N(\mu)| \leq \Delta_N^s(\mu),$$

where

$$\Delta_N^s(\mu) \equiv \frac{\|\ell(\cdot)\|_{X'} \|r(\cdot;\mu)\|_{X'}}{\beta^{\mathrm{LB}}(\mu)},$$

and $\|\cdot\|_{X'}$ refers to the dual norm with respect to $X^{\mathcal{N}}$. □

The proof is based on arguments provided in [11, 18].

It is clear that the quality of the error bound will depend on the quality of the inf-sup lower bound. In particular, we note that in the more conventional error estimate the denominator is given by $\beta(\mu)$; we recover this result only as $\mu \to \bar{\mu}^{k^*}$ — corresponding to relatively small subdomains and hence large K. However, we can ensure reasonable accuracy by choosing

$$\varphi(\mu, \bar{\mu}) = \delta \frac{\tilde{\beta}(\mu)}{\beta(\bar{\mu})}; \tag{6}$$

here $\delta \in (0, 1)$ is an accuracy control parameter and $\tilde{\beta}(\mu)$ is any (preferably cheap) approximation to $\beta(\mu)$. A good option is $\tilde{\beta}(\mu) \equiv \beta^{\mathrm{UB}}_{\mathrm{SCM}^2}(\mu)$, where $\beta^{\mathrm{UB}}_{\mathrm{SCM}^2}(\mu)$ is the classical SCM^2 *upper* bound for $\beta(\mu)$ valid over all of $\mathcal{D}$: the SCM^2 upper bound is (diabolically) very accurate compared to the SCM^2 lower bound, and can be constructed "along side" our natural–norm SCM lower bound at relatively little additional cost — and only in the Offline stage. We note that since $g^{\mathrm{LB}}_{\bar{\mu}}(\bar{\mu}; \mathcal{C}_{\bar{\mu}}) = 1$, the greedy algorithm is guaranteed to converge for any $\varphi(\mu, \bar{\mu}) < 1$ — although $\varphi(\mu, \bar{\mu})$ close to 1 may necessitate a large number ($K \gg 1$) of small subdomains. In actual practice at least for the Helmholtz equation $\bar{\beta}_{\bar{\mu}}(\mu)$ is a very good approximation to, and in fact often exactly equal to, $\beta_{\bar{\mu}}(\mu)$, in which case we may plausibly choose $\varphi = 0$.

Let us now summarize the Offline–Online procedure for the natural–norm SCM. First define

$$n_{\mathrm{greedy}} = \sum_{k=1}^{K} \left(J_{\bar{\mu}^k} + 1 \right),$$

and

$$J^{\max} = \max_{1 \leq k \leq K} J_{\bar{\mu}^k};$$

also denote by n_{train} the cardinality of Ξ. Let n_{eig} denote the number of truth eigenproblems; for the natural norm SCM we have

$$n_{\mathrm{eig}} = Q + \sum_{k=1}^{K} \left(J_{\bar{\mu}^k} + 1 \right).$$

In the Offline stage we must execute the greedy: we must solve n_{eig} truth eigenproblems over $X^{\mathcal{N}}$; we must perform $n_{\mathrm{greedy}} n_{\mathrm{train}}$ LP's — in Q variables

with at most $2Q + J^{\max}$ constraints — for the lower bounds; and we must perform $\mathrm{O}(n_{\text{greedy}} n_{\text{train}} Q)$ evaluations for the upper bounds. If we invoke the SCM^2 upper bound for $\tilde{\beta}$ in (6) we incur an additional cost of $n_{\text{greedy}} n_{\text{train}} Q(Q+1)/2$ operations, as described in the next paragraph. Only the operation count for the first item — solution of the eigenproblems — will depend on $\mathcal{N}$. Most relevant to the current paper, the natural–norm SCM will typically greatly reduce both n_{eig} and n_{greedy} relative to previously proposed techniques. In the Online stage we approximate $k^*(\mu)$ by a search over a few $\bar{\mu} \in S$ near μ: we must thus perform O(1) LP's in Q variables with at most $2Q + J^{\max}$ constraints — independent of $\mathcal{N}$.

In Sections 4 and 5 we shall frequently compare the (Online and Offline) computational effort for the natural–norm SCM and the classical SCM^2, and hence we now briefly discuss SCM^2. First, we let M_β and M_+ refer to the numbers of neighboring points used to impose the SCM^2 stability and positivity constraints, respectively, and we set $\widehat{Q} = Q(Q+1)/2$ [7]. We denote the SCM^2 lower bound and upper bound as $\beta^{\text{LB}}_{\text{SCM}^2}(\mu)$ and $\beta^{\text{UB}}_{\text{SCM}^2}(\mu)$, respectively. In the Offline stage we require: (i) $n_{\text{eig}} = 2\widehat{Q} + J_{\text{SCM}^2}$ truth eigenproblems, (ii) $n_{\text{train}} J_{\text{SCM}^2}$ LPs with $\widehat{Q}$ variables and $2\widehat{Q} + M_\beta + M_+$ constraints for the lower bound, and (iii) $n_{\text{train}} J_{SCM^2} \widehat{Q}$ operations for the upper bound. In the Online stage, the SCM^2 lower bound requires an LP with (again) $\widehat{Q}$ variables and $2\widehat{Q} + M_\beta + M_+$ constraints.

4 Examples: The Helmholtz Equation

We first define some general Helmholtz terminology that will be of use subsequently. We restrict attention to two parameters ($P = 2$). In particular, we consider $a(w, v; \mu) = \mathcal{A}(w, v; \mu) - \omega^2 \mathcal{M}(w, v; \mu)$, where $\mathcal{A}$ is independent of ω^2, $\mathcal{A}$ is coercive and continuous over X, and $\mathcal{M}$ is coercive and continuous over $L^2(\Omega)^{\mathcal{V}}$. If ω^2 is a parameter in the problem under consideration, we set $\mu = (\rho = \mu_1, \omega^2 = \mu_2)$, otherwise we set $\rho = \mu$; then we introduce an eigenproblem for $(\chi^i(\rho) \in X^{\mathcal{N}}, \lambda^i(\rho) \in \mathbb{R}_+), 1 \le i \le \mathcal{N}$:

$$\mathcal{A}(\chi^i(\rho), v; \rho) = \lambda^i(\rho) \mathcal{M}(\chi^i(\rho), v; \rho), \forall v \in X^{\mathcal{N}},$$

ordered such that $0 < \lambda^1(\rho) \le \lambda^2(\rho) \le \cdots \lambda^{\mathcal{N}}(\rho)$. Clearly any $\mathcal{D}$ that does not include any "resonances" $\omega^2 = \lambda^i(\rho), 1 \le i \le \mathcal{N}$, shall honor our well–posedness assumption.

4.1 Anisotropic Wavespeed

Let us first consider the particular scalar ($\mathcal{V} = 1$) Helmholtz example on the unit square Ω with homogeneous Dirichlet boundary conditions on the bottom boundary Γ_B. This problem takes the form: find $w \in X^{\mathcal{N}}$ satisfying

$$\int_\Omega \frac{\partial w}{\partial x_1} \frac{\partial v}{\partial x_1} + \mu_1 \int_\Omega \frac{\partial w}{\partial x_2} \frac{\partial v}{\partial x_2} - \mu_2 \int_\Omega wv = \int_\Omega fv, \qquad \forall v \in X^{\mathcal{N}}, \qquad (7)$$

where f is a forcing function (irrelevant in the present context) and our function space is given by $X^{\mathcal{N}} \subset \{v \in H^1(\Omega) | v_{\Gamma_B} = 0\}$. The first parameter is related to an anisotropic wavespeed and the second parameter is the reduced frequency squared, hence from the discussion above $\rho = \mu_1$ and $\omega^2 = \mu_2$. It follows from (7) that $\mathcal{V} = 1$, $P = 2$, and that we have an affine decomposition with $Q = 3$: $\Theta_1(\mu) = 1, \Theta_2(\mu) = \mu_1, \Theta_3(\mu) = -\mu_2$, and

$$a_1(w,v) = \int_\Omega \frac{\partial w}{\partial x_1}\frac{\partial v}{\partial x_1}\,, \quad a_2(w,v) = \int_\Omega \frac{\partial w}{\partial x_2}\frac{\partial v}{\partial x_2}\,, \quad a_3(w,v) = \int_\Omega wv\,.$$

Note that $\Theta_q, 1 \le q \le Q$, are affine functions of μ.

Assume that our truth approximation is of tensor product form such that the discrete problem remains separable. In this case it is simple to demonstrate by explicit calculation that for any connected $\mathcal{D}_{\bar{\mu}}$ which does not include any resonances (hence between two resonance lines)

$$\bar{\beta}_{\bar{\mu}}(\mu) = \beta_{\bar{\mu}}(\mu), \forall \mu \in \mathcal{D}_{\bar{\mu}};$$

it thus follows from Proposition 2 that for any such $\mathcal{D}_{\bar{\mu}}$ our lower bound (2) will in fact be positive over the convex hull of $\mathcal{C}_{\bar{\mu}}$. In this particular case we observe that $\mathcal{D}_{\bar{\mu}}$ may be quite large and that we will require only a relatively small sample $\mathcal{C}_{\bar{\mu}}$ to construct a good lower bound. For this problem, neither cautionary note of Section 3.1 is relevant.

We consider the parameter domain $\mathcal{D} \subset [0.8, 1.2] \times [10, 50]$ shown in Figure 1: the domain contains 5 unconnected regions separated by 4 resonances — note that in this case each resonance is simply a straight line. To begin we create an optimal lower bound "by hand": we introduce $K = 5$ subdomains — a subdomain for each unconnected quadrangular region; for each subdomain $1 \le k \le K$ we choose $\mathcal{C}^{\bar{\mu}^k}$ as the four corners of the subdomain supplemented by two interior points and the point $\bar{\mu}^k$ — hence $J_{\bar{\mu}^k} = 7$. The points are illustrated in Figure 1. We summarize the resulting lower bound in Figure 3(a) as a histogram of $\beta^{\rm LB}(\mu)/\beta(\mu)$ constructed from a random uniform sample $\Xi_{\rm test}$ over $\mathcal{D}$ of size 441.

Let us now apply our greedy strategy for $\epsilon_{\bar{\beta}} = 0.75$, $n_{\rm train} = 5000$, and $\varphi = 0$: we obtain $K = 12$,

$$J_{\bar{\mu}^k, k=1,\ldots,12} = [14, 10, 8, 18, 12, 2, 2, 2, 2, 2, 2, 1],$$

and $n_{\rm eig} = 90$. The first five subdomains actually correspond to the five regions in between the resonances: these five subdomains cover almost the entire domain $\mathcal{D}$ — and in fact largely capture the five unconnected components of $\mathcal{D}$; the final seven subdomains are "patches" — each contains either one or two $\hat{\mu}_{\bar{\mu}^\cdot}$ points quite near a resonance. The subdomains and points are illustrated in Figure 2; the histogram for the greedy is shown in Figure 3(b). We observe that the greedy performs quite well relative to (in fact, arguably better than) the "by hand" construction.

As a comparison, we have applied the classical SCM^2 method on the same train sample set for the choice $M_\beta = 16$ ($M_+ = 0$). We obtain $n_{\rm eig} = 2643$:

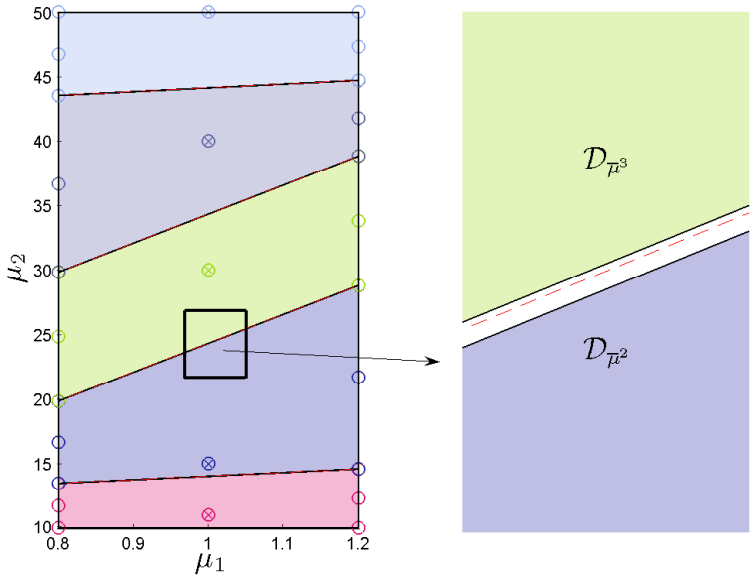

Figure 1: Anisotropic wavespeed problem ("by hand"): Parameter domain $\mathcal{D}$ ($\times$ denotes $\bar{\mu}$ and $\circ$ denotes $\hat{\mu}$ associated to a $\mathcal{C}_{\bar{\mu}}$); dashed lines indicate resonances.

much larger Offline effort, and (since $M_\beta > J^{\max}$) larger Online effort as well — in particular since the classical SCM[2] involves $\widehat{Q} = Q(Q+1)/2$ terms in the objective function and $2\widehat{Q} + M_\beta$ constraints.

4.2 "Microphone" Problem

Consider the simple acoustics microphone probe Helmholtz problem ($\mathcal{V} = 1$) as described in [7, 18]. The original domain $\Omega^o(L)$ is a channel probe inlet followed by a microphone plenum cavity of height $1/4 + L$ as shown in Figure 4(a). The (fixed, parameter independent) mapped domain is given by $\Omega = \Omega(L_{\text{ref}} = 1) = [-1/2, 1] \times [0, 1/4] (\equiv \Omega_{\text{bot}}) \cup [0, 1] \times [1/4, 5/4] (\equiv \Omega_{\text{top}})$. We impose Dirichlet conditions on the left boundary Γ_{in} of Ω. Our function space is thus given by $X^{\mathcal{N}} \subset \{v \in H^1(\Omega) | v_{\Gamma_{\text{in}}} = 0\}$. The two parameters, $\mu_1 = L$ and $\mu_2 = \omega^2$, correspond to the height of the microphone plenum (Ω_{top}) and the reduced frequency squared, respectively (hence again $\rho = \mu_1$, $\omega^2 = \mu_2$). The parameter range $\mathcal{D} = [0.3, 0.6] \times [3.0, 6.0]$ lies between the first and second resonance lines, as shown in Figure 5.

The affine formulation is recovered for $Q = 5$, with $\Theta_1(\mu) = 1$, $\Theta_2(\mu) = -\mu_2$, $\Theta_3(\mu) = \mu_1$, $\Theta_4(\mu) = 1/\mu_1$, $\Theta_5(\mu) = -\mu_1\mu_2$, and

$$a_1(w, v) = \int_{\Omega_{\text{bot}}} \nabla w \cdot \nabla v, \; a_2(w, v) = \int_{\Omega_{\text{bot}}} wv, \; a_3(w, v) = \int_{\Omega_{\text{top}}} \frac{\partial w}{\partial x_1} \frac{\partial v}{\partial x_1},$$

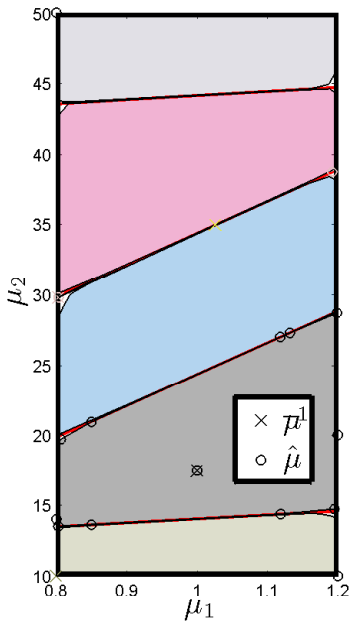

Figure 2: Anisotropic Wavespeed problem (greedy): Subdomains and the set $\mathcal{C}_{\bar{\mu}^1}$.

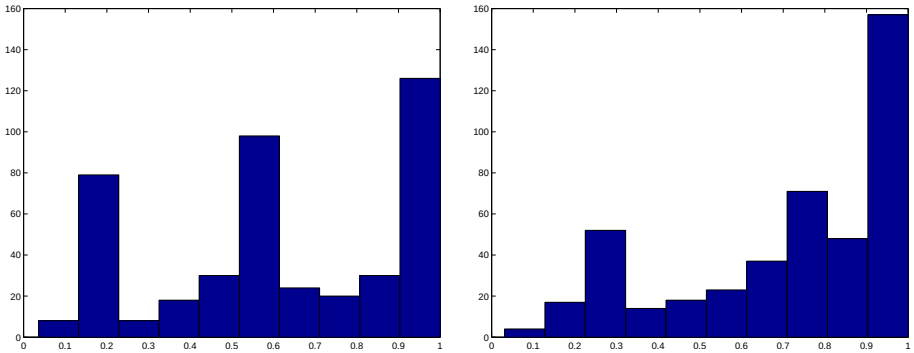

Figure 3: Histograms of $\beta^{\mathrm{LB}}(\mu)/\beta(\mu)$ for anisotropic wavespeed problem: (a) "by hand," $\min_{\mu\in\Xi_{\mathrm{test}}} \frac{\beta^{\mathrm{LB}}(\mu)}{\beta(\mu)} = 0.036$, $\mathrm{avg}_{\mu\in\Xi_{\mathrm{test}}} \frac{\beta^{\mathrm{LB}}(\mu)}{\beta(\mu)} = 0.616$; (b) greedy, $\min_{\mu\in\Xi_{\mathrm{test}}} \frac{\beta^{\mathrm{LB}}(\mu)}{\beta(\mu)} = 0.031$, $\mathrm{avg}_{\mu\in\Xi_{\mathrm{test}}} \frac{\beta^{\mathrm{LB}}(\mu)}{\beta(\mu)} = 0.720$.

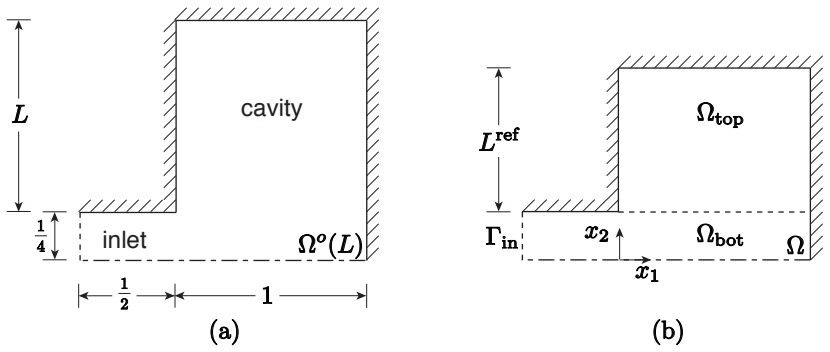

Figure 4: Microphone problem: (a) Original domain, and (b) Mapped domain.

$$a_4(w,v) = \int_{\Omega_{\rm top}} \frac{\partial w}{\partial x_2}\frac{\partial v}{\partial x_2},\ a_5(w,v) = \int_{\Omega_{\rm top}} wv.$$

(The inner product is chosen to be the same as in [7].) Note that as is usually the case for problems with parametrized geometry, the $\Theta_q,\ 1 \le q \le Q$, are no longer affine functions of μ.

Let us apply our greedy strategy for $\epsilon_{\bar\beta} = 0.75$, $n_{\rm train} = 5000$, and $\varphi = 0$: we obtain $K = 1$ and $J_{\bar\mu^1} = 5$ corresponding to $n_{\rm eig} = 11$. The result is considered "ideal": the single required subdomain includes only the four corner points of the parameter domain and $\bar\mu^1$. We plot $\beta(\mu)$ and $\beta^{\rm LB}(\mu)$ for a sample of 1681 points in $\mathcal{D}$ in Figure 6; we present in Figure 7(a) the histogram of $\beta^{\rm LB}(\mu)/\beta(\mu)$ constructed from a random uniform sample $\Xi_{\rm test}$ over $\mathcal{D}$ of size 441. We observe that the inf-sup quality is rather good even for the non-stringent tolerance $\varphi = 0$.

This problem is solved by the classical SCM^2 in [7]. The new natural–norm SCM requires less effort than the classical SCM^2 in both the Offline and Online stages: in the Offline stage, the classical SCM^2 requires from $n_{\rm eig} = 52$ — for the "minimized Offline cost" choice $M_\beta = \infty$ — to $n_{\rm eig} = 128$ — for the "minimized Online cost" choice $M_\beta = 4$; in the Online stage, even for the "minimized Online cost" setting, the classical SCM^2 requires more computational effort than the natural–norm SCM due to the $O(Q^2)$ terms in the inf-sup expansion of the former. The histogram of $\beta^{\rm LB}_{\rm SCM^2}(\mu)/\beta(\mu)$ (using the "minimized Online cost" setting) for the same set $\Xi_{\rm test}$ as above is shown in Figure 7(b) — a modest improvement over the ($\varphi = 0$) natural–norm SCM. (We shall consider $\varphi \neq 0$ in several later examples.)

4.3 The Hole-in-Block Problem

We consider a Helmholtz acoustics problem ($\mathcal{V} = 1$) which corresponds to a hole in a square block as shown in Figure 8. The domain is given by $\Omega^o(h) = [0,1]\times[0,1]\backslash[h, h+1/4]\times[1/4, 3/4]$, where h is the parameter to control the position of the rectangular hole. We choose $h_{\rm ref} = 3/8$ for our mapped/reference

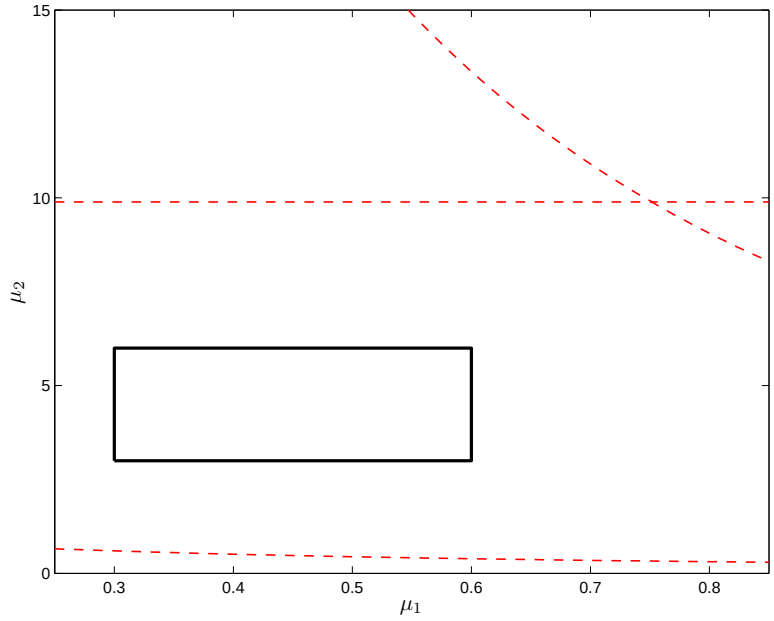

Figure 5: Microphone problem: Parameter domain $\mathcal{D}$; dashed lines indicate resonances.

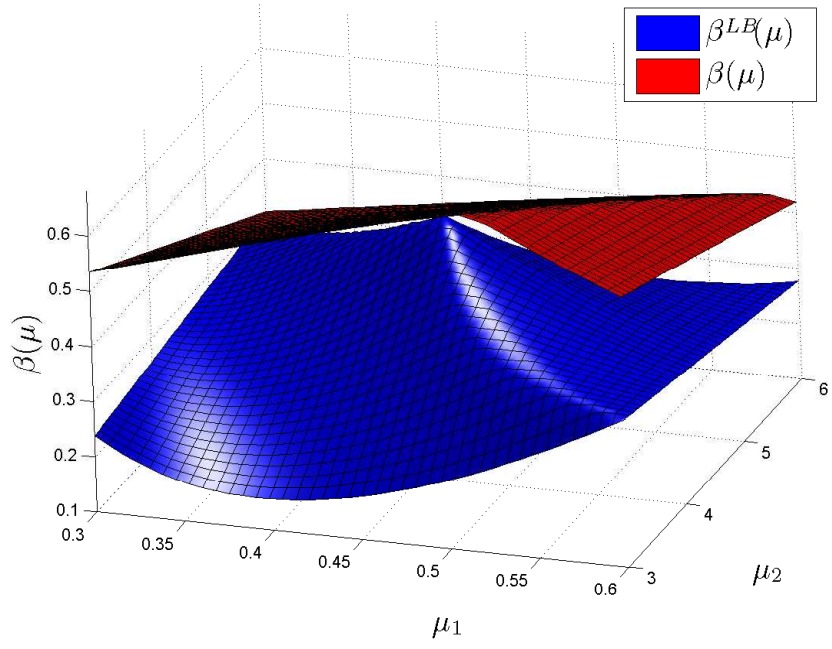

Figure 6: Microphone problem: $\beta(\mu)$ and $\beta^{\mathrm{LB}}(\mu)$.

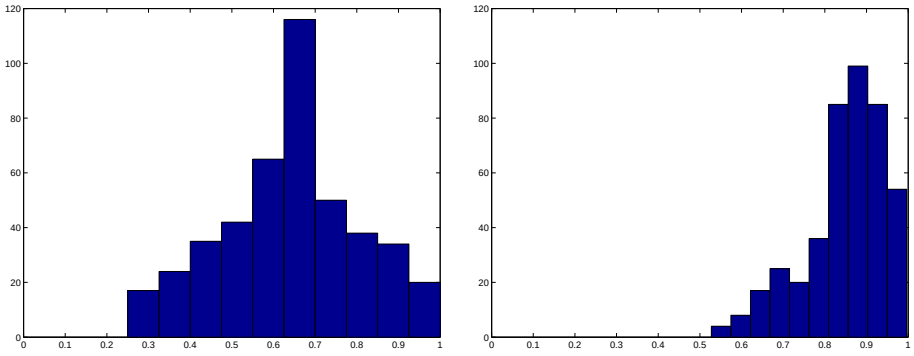

Figure 7: Microphone problem: Histogram for $\Xi_{\rm test}$ of (a) $\beta^{\rm LB}(\mu)/\beta(\mu)$; $\min_{\mu\in\Xi_{\rm test}} \frac{\beta^{\rm LB}(\mu)}{\beta(\mu)} = 0.250$, $\text{avg}_{\mu\in\Xi_{\rm test}} \frac{\beta^{\rm LB}(\mu)}{\beta(\mu)} = 0.639$, and (b) $\beta^{\rm LB}_{\rm SCM^2}(\mu)/\beta(\mu)$; $\min_{\mu\in\Xi_{\rm test}} \frac{\beta^{\rm LB}_{\rm SCM^2}(\mu)}{\beta(\mu)} = 0.528$, $\text{avg}_{\mu\in\Xi_{\rm test}} \frac{\beta^{\rm LB}_{\rm SCM^2}(\mu)}{\beta(\mu)} = 0.848$.

domain. We impose Dirichlet conditions on Γ_4, Γ_5 and Γ_6, and hence our function space is given by $X^{\mathcal{N}} \subset X = \{v \in H^1(\Omega) | v_{\Gamma_{4,5,6}} = 0\}$. Our $P = 2$ parameters are $\mu_1 = h$ and $\mu_2 = \omega^2$ (so that $\rho = \mu_1$ here); the parameter domain $\mathcal{D} = [1/8, 5/8] \times [11/2, 23/2]$ lies in between the first and second resonance lines, as shown in Figure 9.

In this case, the identification of the geometric transformations and associated affine representation are already cumbersome, and we thus appeal to the automatic procedures available in the rbMIT© pre–processor [6]. In this particular case, we obtain

$$\Theta_1(\mu) = 3/(6 - 8\mu_1),\ \Theta_2(\mu) = 3/(8\mu_1),\ \Theta_3(\mu) = 1,$$

$$\Theta_4(\mu) = \mu_1,\ \Theta_5(\mu) = \mu_2,\ \Theta_6(\mu) = -\mu_1\mu_2;$$

note again that in the presence of parametrized geometry, we obtain $\Theta_q, 1 \le q \le Q$ that are not affine functions of μ. We omit the corresponding $a_q, 1 \le q \le Q$ — integrals of bilinear forms over restricted subdomains of Ω — in the interest of brevity.

We apply our greedy strategy for $\epsilon_{\bar\beta} = 0.75$, $n_{\rm train} = 5000$, and $\varphi = 0$: we obtain $K = 2$ and $J_{\bar\mu^k, k=1,2} = [35, 5]$ corresponding to $n_{\rm eig} = 48$. Note that the first subdomain covers almost the entirety of $\mathcal{D}$, as shown in Figure 9; the second domain acts as a "patch" for the regions near the resonances. The histogram of $\beta^{\rm LB}(\mu)/\beta(\mu)$ constructed from a random uniform sample $\Xi_{\rm test}$ over $\mathcal{D}$ of size 441 is shown in Figure 10(a). We observe reasonably good quality — certainly sufficient in the reduced basis error estimation context.

As a comparison, we have applied the classical SCM^2 method on the same train set for the choice $M_\beta = 16$. We obtain $n_{\rm eig} = 1527$: the classical SCM^2 approach is roughly 32 times slower than the natural–norm SCM in the Offline

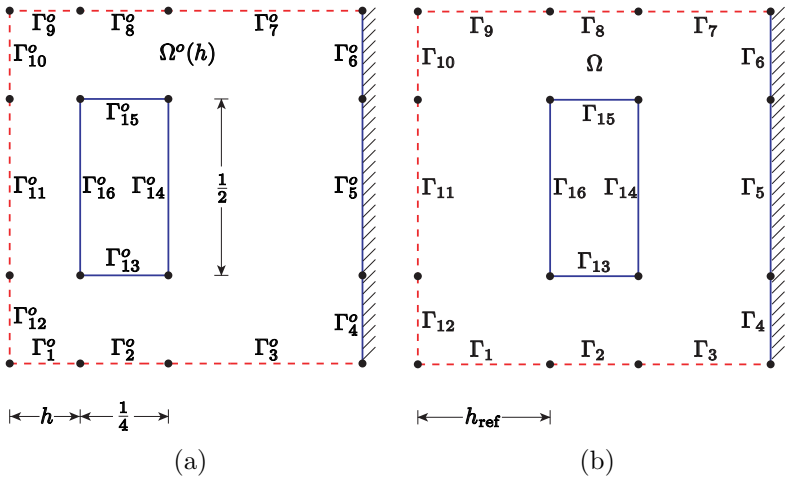

Figure 8: Hole-in-Block problem: (a) Original domain, and (b) Mapped domain.

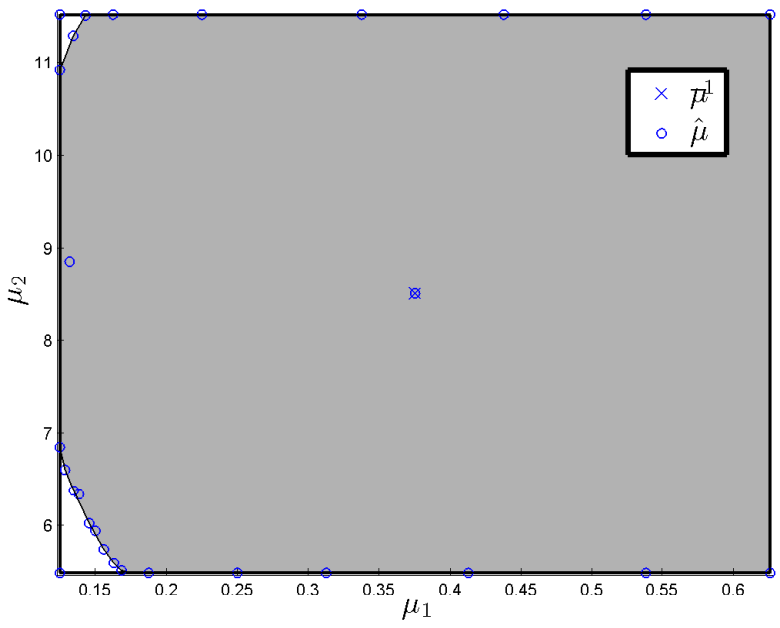

Figure 9: Hole-in-Block problem: The first subdomain (shaded) and $\mathcal{C}_{\bar{\mu}^1}$.

stage. We present in Figure 10(b) the histogram of $\beta^{\rm LB}_{\rm SCM^2}(\mu)/\beta(\mu)$ for the same set $\Xi_{\rm test}$ as above; note that negative $\beta^{\rm LB}_{\rm SCM^2}(\mu)$ is set to zero in this example. It is seen that the SCM^2 fails to provide a "good" (strictly positive) inf-sup lower bound for 100 points in the set $\Xi_{\rm test}$, even though the train sample Ξ is much larger than the test sample $\Xi_{\rm test}$. Further tests on several random $\Xi_{\rm test}$ sets indicate that the probability of obtaining strictly positive SCM^2 inf-sup lower bound is approximately 0.75, as suggested by Figure 10(b). The SCM^2 result can be improved somewhat by increasing $n_{\rm train}$; however, since the SCM^2 is only providing coverage in small neighborhoods of the train points, it is unlikely that we can obtain complete positivity coverage over $\mathcal{D}$.

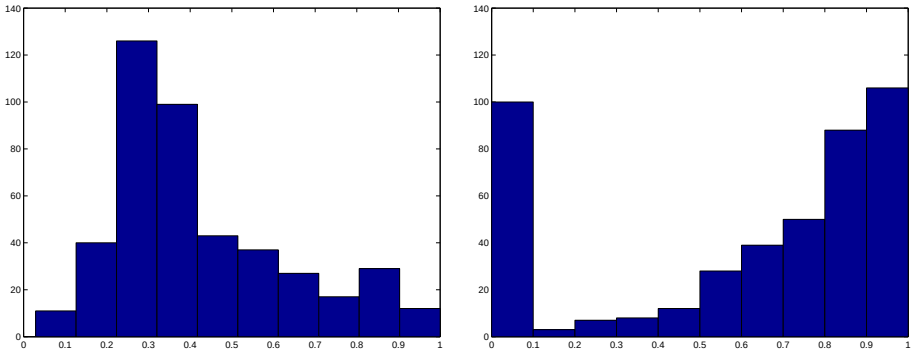

Figure 10: Hole-in-Block problem: Histogram for $\Xi_{\rm test}$ of (a) $\beta^{\rm LB}(\mu)/\beta(\mu)$; $\min_{\mu\in\Xi_{\rm test}} \frac{\beta^{\rm LB}(\mu)}{\beta(\mu)} = 0.029$, $\text{avg}_{\mu\in\Xi_{\rm test}} \frac{\beta^{\rm LB}(\mu)}{\beta(\mu)} = 0.425$, and (b) $\beta^{\rm LB}_{\rm SCM^2}(\mu)/\beta(\mu)$; $\min_{\mu\in\Xi_{\rm test}} \frac{\beta^{\rm LB}_{\rm SCM^2}(\mu)}{\beta(\mu)} = 0$, $\text{avg}_{\mu\in\Xi_{\rm test}} \frac{\beta^{\rm LB}_{\rm SCM^2}(\mu)}{\beta(\mu)} = 0.600$.

4.4 The Center Crack Problem

We consider a Helmholtz linear elasticity problem ($\mathcal{V} = 2$) which corresponds to a plate containing an internal center crack of length $2b$ under "Mode I" tension. In consideration of the symmetry of geometry and loading, we consider only a quarter of the original domain as shown in Figure 11: $\Omega(b) = [0,1] \times [0,2]$ and Ω (the mapped domain) $= \Omega(b_{\rm ref} = 1/2)$; note that the crack corresponds to the boundary Γ_1. We model the plate as plane-stress linear isotropic with (scaled) unity density, unity Young's modulus, and Poisson ratio $\nu = 0.3$. We impose a vertical oscillatory uniform force of frequency ω on the top boundary Γ_4; symmetric boundary conditions on Γ_2 and Γ_5; and stress-free conditions on Γ_1 and Γ_3. Our function space is then given by $X^{\mathcal{N}} \subset X \equiv \{(v_1, v_2) \in (H^1(\Omega))^2 \,|\, v_1|_{\Gamma_2} = 0, v_2|_{\Gamma_5} = 0\}$. Our $P = 2$ parameters are $\mu_1 = b$ and $\mu_2 = \omega^2$ (so that $\rho = \mu_1$); the parameter domain $\mathcal{D} = [1/5, 4/5] \times [3/5, 9/5]$ lies in between the first and second resonance lines, as shown in Figure 12. In this case, the problem satisfies the affine decomposition for $Q = 8$, which

is generated automatically by the software package rbMIT©[6]; the functions $\Theta_q(\mu), 1 \le q \le Q$, are not affine in μ.

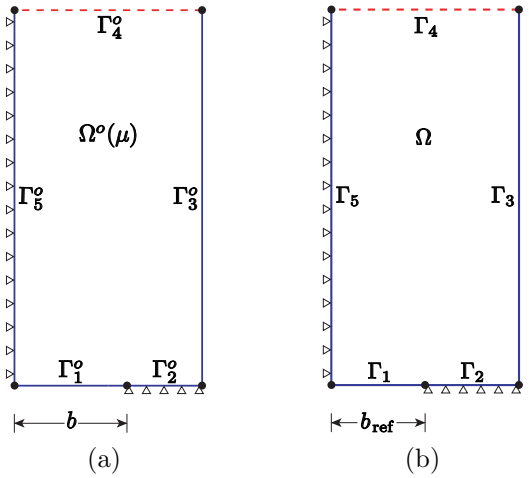

Figure 11: Center crack problem: (a) Original domain, and (b) Mapped domain.

The greedy strategy is applied for $\epsilon_{\bar{\beta}} = 0.75$, $n_{\text{train}} = 10^4$, and $\varphi = 0$: we obtain $K = 9$ and $J_{\bar{\mu}^k, k=1,\ldots,9} = [83, 31, 19, 13, 10, 7, 5, 6, 3]$ corresponding to $n_{\text{eig}} = 194$. Note that the first subdomain covers almost the entirety of $\mathcal{D}$, as shown in Figure 12. The histogram of $\beta^{\text{LB}}(\mu)/\beta(\mu)$ constructed from a random uniform sample Ξ_{test} over $\mathcal{D}$ of size 441 is shown in Figure 13. The clustering of points near the resonances is obviously less than desirable, and will be even more limiting in higher parameter dimension. However, the natural-norm SCM does nevertheless greatly improve over the SCM^2.

In this case the classical SCM^2 approach is not viable — we require many thousands of truth eigenvalue solutions just to achieve a positive inf-sup lower bound over a modest train sample.

4.5 Electromagnetic Cavity Problem

We consider Maxwell's equations in the second order curl-curl formulation: find $E \in X = H_0(\text{curl}; \Omega)$ such that

$$\nabla \times \nu^{-1} \nabla \times E - \varepsilon \omega^2 E = i\omega J^c, \quad x \in \Omega. \tag{8}$$

To keep things simple, we focus on the two-dimensional Maxwell's equation in transverse electric form where $E(x_1, x_2) = (E_1, E_2)$ is the electric vector field, $J^c = (J_1^c, J_2^c)$ is the current source and $(\varepsilon(x), \nu(x))$ are the tensors of electric permittivity and magnetic permeability, respectively. To simplify matters, we assume isotropic materials with piecewise constant permittivity and permeability in which case the permittivity and permeability tensors take the form $\varepsilon(x)$I and $\nu(x)$I, respectively, where $\varepsilon(x)$ and $\nu(x)$ are piecewise constant scalars and

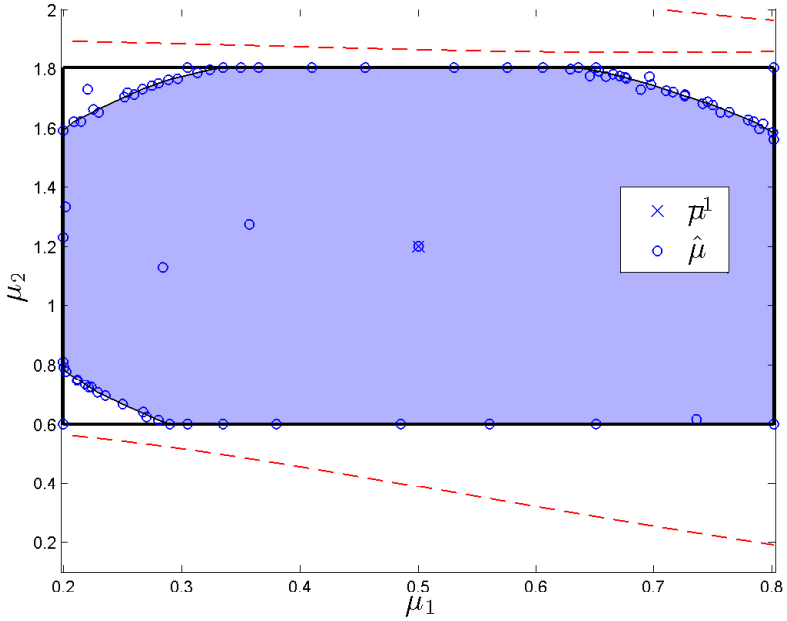

Figure 12: Center crack problem: The first subdomain (shaded) and $\mathcal{C}_{\bar{\mu}^1}$; dashed lines indicate resonances.

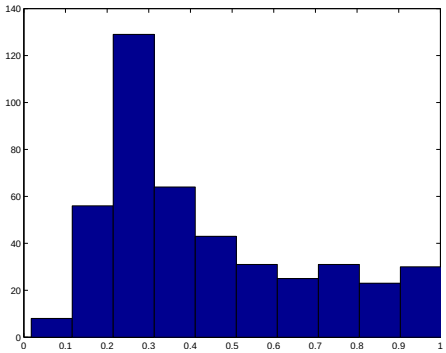

Figure 13: Center crack problem: Histogram of $\beta^{\mathrm{LB}}(\mu)/\beta(\mu)$ for Ξ_{test}; $\min_{\mu\in\Xi_{\mathrm{test}}} \frac{\beta^{\mathrm{LB}}(\mu)}{\beta(\mu)} = 0.018$, $\mathrm{avg}_{\mu\in\Xi_{\mathrm{test}}} \frac{\beta^{\mathrm{LB}}(\mu)}{\beta(\mu)} = 0.438$.

I is the identity matrix. Finally ω, set to $5\pi/2$ for this example, reflects the angular frequency of the electromagnetic wave.

We seek the solution to this problem in the closed geometry illustrated in Figure 14 in which we assume all exterior boundaries to be perfectly electrically conducting with vanishing tangential electric fields. The cavity is loaded with two materials, each occupying half of the cavity. For simplicity we assume that Ω_1 of the cavity is vacuum so that $\varepsilon_1 = \nu_1 = 1$ while the material parameters in Ω_2 are the parameters of the problem, i.e. $\mu = (\varepsilon_2, \nu_2)$. See [3] and the references therein for the formulation and analysis of the discontinuous Galerkin method we are using for this test problem. It is well known that for this problem there are curved resonance lines, which means that this is a challenging problem for the natural-norm SCM. The parameter domain is set to $\mathcal{D} = [2.75, 3.15] \times [1.01, 1.19]$, which is between resonances as shown in Figure 15.

In this setting (8) results in the bilinear form $a(u, v)$

$$a(u,v) = \left(\nu^{-1}\nabla \times u, \nabla \times v\right)_\Omega - \omega^2 \left(\varepsilon u, v\right)_\Omega ,$$

which gives the following affine decomposition for $Q = 3$: $\Theta_1(\mu) = 1$, $\Theta_2(\mu) = \nu_2^{-1}$, $\Theta_3(\mu) = \varepsilon_2$, and

$$\begin{aligned} a_1(u,v) &= \nu_1^{-1} \left(\nabla \times u, \nabla \times v\right)_{\Omega_1} - \omega^2 \varepsilon_1 \left(u, v\right)_{\Omega_1} , \\ a_2(u,v) &= \left(\nabla \times u, \nabla \times v\right)_{\Omega_2} , \\ a_3(u,v) &= -\omega^2 \left(u, v\right)_{\Omega_2} . \end{aligned}$$

Here $(\cdot,\cdot)_\Omega$ refers to the L^2 inner product restricted to Ω.

We apply the natural norm SCM greedy algorithm for $\epsilon_{\bar{\beta}} = 0.75$, $n_{\text{train}} = 2145$, and $\varphi = 0$ to obtain $K = 2$, $J_{\bar{\mu}^k, k=1,2} = [7, 3]$ and $n_{\text{eig}} = 15$. Figure 16 shows the distribution of $\mathcal{C}_{\bar{\mu}^1}$: $\mathcal{R}_{\bar{\mu}^1}$, of size 2109, covers almost the entirety of $\mathcal{D}$. This subdomain is almost "ideal": except the (starting) first point and the third point (which is outside of $\mathcal{R}_{\bar{\mu}^1}$ and has negative $\bar{\beta}_{\bar{\mu}_1}(\mu)$), all the other points are corner points of the polygon. The second subdomain is just a small patch. To visualize the lower bound, we compute the true inf-sup constant for a sample of 2100 points in $\mathcal{D}$ and plot $\beta(\mu)$ and $\beta^{\text{LB}}(\mu)$ in Figure 17. We can see that in this case the lower bound is rather pessimistic along the intersection line of the two subdomains: our greedy algorithm is "too greedy" in this example.

Thus, we consider a second test with a nonzero inf-sup tolerance function $\varphi(\mu, \bar{\mu})$ defined by (6) with $\tilde{\beta}(\mu) \equiv \beta^{\text{UB}}_{\text{SCM}^2}(\mu)$ and $\delta = 0.2$. In this second test case, we obtain $K = 4$, $J_{\bar{\mu}^k, k=1,2,3,4} = [7, 4, 4, 2]$ and $n_{\text{eig}} = 24$. The set $\mathcal{C}_{\bar{\mu}^1}$ does not change, but we obtain a slightly smaller subdomain $\mathcal{R}_{\bar{\mu}^1}$; the remaining three subdomains are all just small patches. We plot the resulting $\beta(\mu)$ and $\beta^{LB}(\mu)$ in Figure 18: the exceptionally small values of the inf-sup LB are eliminated.

Figure 19 shows histograms of $\beta^{\text{LB}}(\mu)/\beta(\mu)$ for the two cases considered above ($\delta = 0$ and $\delta = 0.2$) — at the expense of 9 more Offline eigenproblems, we obtain a noticeable improvement in accuracy with $\delta = 0.2$.

We also apply the classical SCM^2 for the same train set and with $M_\beta = 20$, $M_+ = 6$. We obtain $n_{\text{eig}} = 212$ — a factor of roughly 14 (respectively, 9) increase

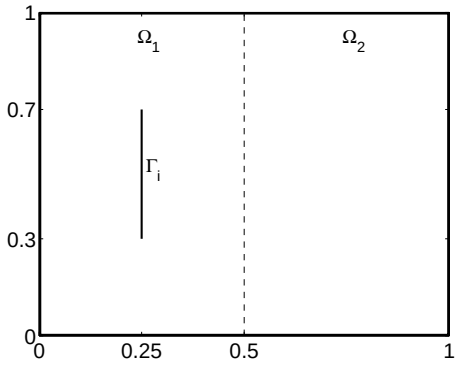

Figure 14: Geometry of the Electromagnetic Cavity Problem.

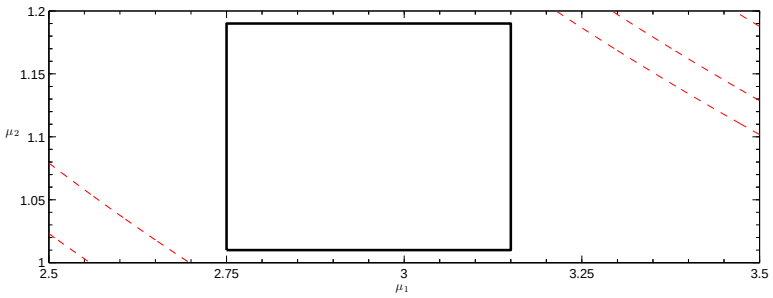

Figure 15: The parameter domain for the Electromagnetic Cavity Problem.

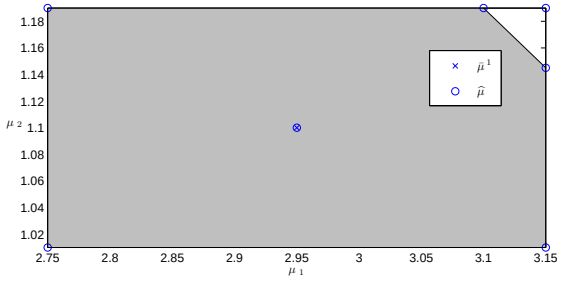

Figure 16: Electromagnetic Cavity problem: The first subdomain (shaded) and $\mathcal{C}_{\bar{\mu}^1}$.

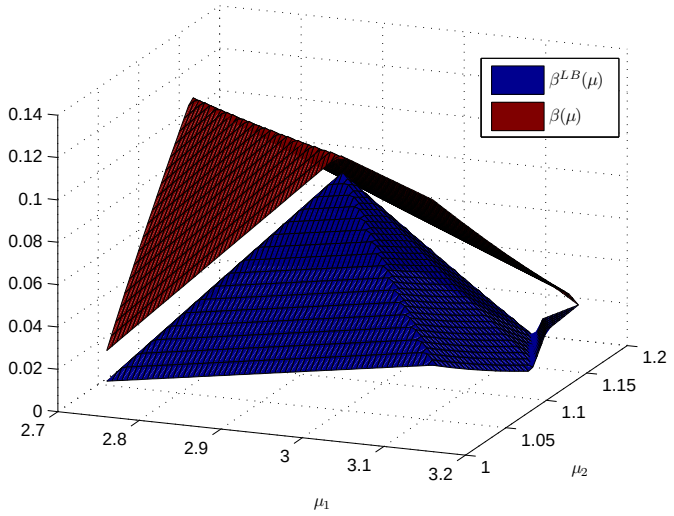

Figure 17: Electromagnetic Cavity problem ($\delta = 0$): $\beta(\mu)$ and $\beta^{\mathrm{LB}}(\mu)$.

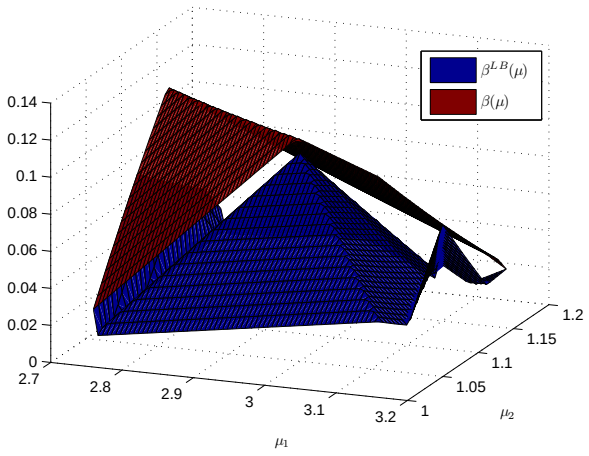

Figure 18: Electromagnetic Cavity problem ($\delta = 0.2$): $\beta(\mu)$ and $\beta^{\mathrm{LB}}(\mu)$.

in the number of Offline eigenproblems compared to the $\delta = 0$ (respectively, $\delta = 0.2$) natural–norm SCM case. Moreover, as observed above, SCM^2 also requires more Online effort since (i) $M_\beta > J^{\max}$ and (ii) the classical SCM inf-sup expansion contains $\widehat{Q}$ terms.

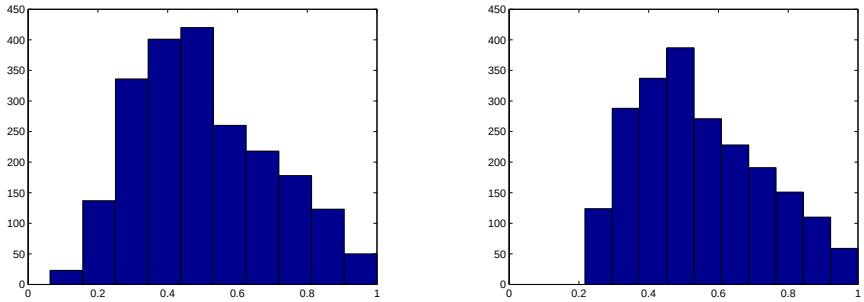

(a) (b)

Figure 19: Electromagnetic Cavity Problem: Histograms of $\beta^{\rm LB}(\mu)/\beta(\mu)$ with (a) $\delta = 0$: $\min_{\mu\in\Xi_{\rm test}} \frac{\beta^{\rm LB}(\mu)}{\beta(\mu)} = 0.063$, $\text{avg}_{\mu\in\Xi_{\rm test}} \frac{\beta^{\rm LB}(\mu)}{\beta(\mu)} = 0.50$ and (b) $\delta = 0.2$: $\min_{\mu\in\Xi_{\rm test}} \frac{\beta^{\rm LB}(\mu)}{\beta(\mu)} = 0.22$, $\text{avg}_{\mu\in\Xi_{\rm test}} \frac{\beta^{\rm LB}(\mu)}{\beta(\mu)} = 0.55$.

5 Convection–Diffusion

Finally, we briefly consider a steady convection–diffusion problem inspired by recent work on applying reduced basis schemes to the Fokker–Planck equation from polymer physics [10]. The steady-state Fokker–Planck equation is a non-coercive convection-diffusion problem — the relevance of the natural–norm SCM in this context is evident. However, for the sake of exposition in the present paper, it is more convenient to consider a simple model convection–diffusion problem that preserves key structural similarities to the Fokker–Planck case. Note also that, unlike the Helmholtz/Maxwell problems considered above, the convection–diffusion problem does not exhibit resonance behavior, and is therefore representative of a separate class of problems.

We consider a scalar ($\mathcal{V} = 1$) convection–diffusion problem on the unit square $\Omega = (0,1)^2$ with homogeneous Dirichlet boundary conditions on $\partial\Omega$. The formulation of this problem is: find $w \in X^{\mathcal{N}} \subset X \equiv H_0^1(\Omega)$ satisfying

$$\mu_1 \int_\Omega \nabla w \cdot \nabla v + \mu_2 \int_\Omega x_1 \frac{\partial w}{\partial x_1} v - \int_\Omega x_2 \frac{\partial w}{\partial x_2} v = \int_\Omega f v, \qquad \forall v \in X^{\mathcal{N}}. \tag{9}$$

Our two parameters are the diffusion coefficient μ_1 and the maximum x_1-velocity μ_2; note our imposed convection velocity is given by $(\mu_2 x_1, -x_2)$. The parameter

domain is taken to be $\mathcal{D} \equiv [0.1, 1] \times [1, 5]$, which corresponds to a Peclet number range of 1 to 50. Note that the problem is coercive on a subset of $\mathcal{D}$ — for example, when $\mu_2 = 1$, the convection velocity $(x_1, -x_2)$ is divergence-free, from which coercivity follows directly — however we have confirmed numerically that coercivity is lost in a subregion of $\mathcal{D}$ corresponding to smaller μ_1 and larger μ_2.

In this case the Offline decomposition is readily identified: $Q = 3$, $\Theta_1(\mu) = \mu_1, \Theta_2(\mu) = \mu_2, \Theta_3(\mu) = -1$, and

$$a_1(w, v) = \int_\Omega \nabla w \cdot \nabla v \,, \quad a_2(w, v) = \int_\Omega x_1 \frac{\partial w}{\partial x_1} v \,, \quad a_3(w, v) = \int_\Omega x_2 \frac{\partial w}{\partial x_2} v \,.$$

Note that the $\Theta_q(\mu)$, $1 \le q \le Q$, are affine functions of μ.

We apply the natural–norm SCM scheme to this convection–diffusion problem with $\epsilon_{\bar{\beta}} = 0.75$, $n_{\text{train}} = 4225$, and φ as in (6) with $\tilde{\beta} = \beta^{\text{UB}}_{\text{SCM}^2}(\mu)$ and $\delta = 0.4$: we obtain $K = 7$, $J_{\bar{\mu}^k, k=1,\ldots,7} = [9, 6, 8, 10, 6, 6, 3]$ and hence $n_{\text{eig}} = 55$. We present in Figure 20 $\beta(\mu)$ and $\beta^{\text{LB}}(\mu)$ for a sample Ξ_{test} of 400 points in $\mathcal{D}$; we provide in Figure 21(a) a histogram of $\beta^{\text{LB}}(\mu)/\beta(\mu)$ for the same set Ξ_{test} of 400 parameter points. We achieve a good approximation over the rather extensive parameter domain.

Finally, we also apply the classical SCM^2 approach with the same train sample and with $M_\beta = 10$. We obtain $n_{\text{eig}} = 36$ in this case: Figure 21(b) shows the histogram of $\beta^{\text{LB}}_{\text{SCM}^2}(\mu)/\beta(\mu)$; we can see that SCM^2 gives a slightly sharper lower bound and with smaller n_{eig}. On the other hand, the natural–norm SCM requires less Online effort since the classical SCM^2 inf-sup expansion contains $\widehat{Q}$ terms. Overall, SCM^2 is the preferred choice for this example since Q is small, however for a problem of this type with $Q \gg 1$ the natural–norm SCM would most likely be preferred.

6 Concluding remarks

The main computational bottleneck in the development of certified reduced basis methods for parametrized partial differential equations remains the need to compute a tight lower bound for the stability parameter, i.e., the inf-sup conditions for non-coercive problems considered here. While there are several past attempts to pursue this, these techniques suffer from significant computational cost, effectively reducing the practicality of these methods to problems with a low dimensional parameter space and simple affine expressions.

In the paper we have, in a novel way, combined two previously proposed methods to arrive at a new approach which is significantly faster without impacting the accuracy of the lower bound estimate. Through a number of different examples, we demonstrate a typical Offline reduction of an order of magnitude; also the Online cost is reduced from Q^2 to Q, with Q measuring the complexity of the affine expansion.

It is expected that this dramatic reduction in computational cost will be even more pronounced when considering more complex problems, non-affine

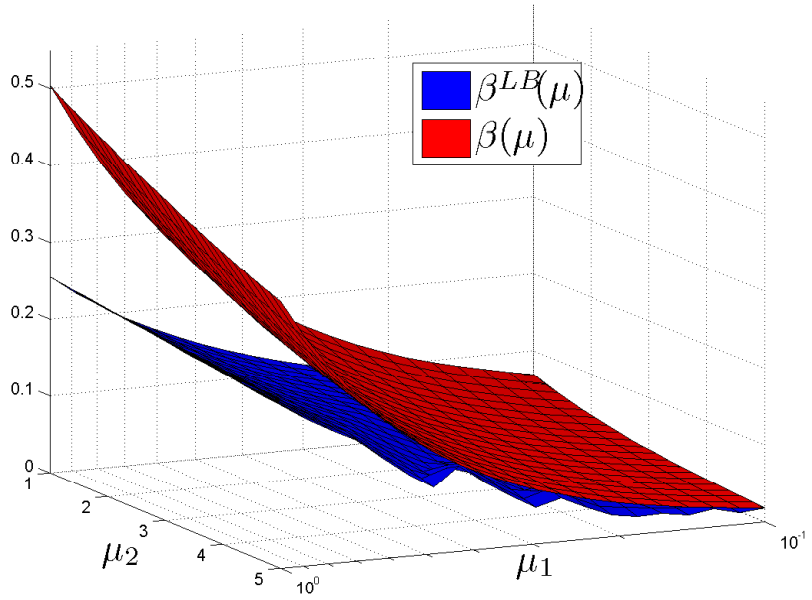

Figure 20: Convection–diffusion problem: $\beta(\mu)$ and $\beta^{\mathrm{LB}}(\mu)$.

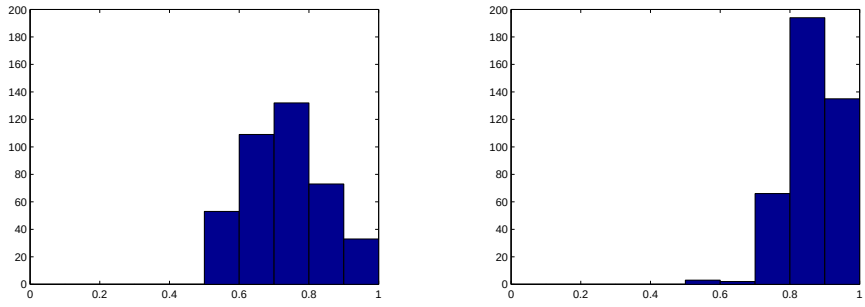

(a) (b)

Figure 21: Convection–diffusion problem: Histogram for Ξ_{test} of (a) $\beta^{\mathrm{LB}}(\mu)/\beta(\mu)$ with $\delta = 0.4$; $\min_{\mu\in\Xi_{\mathrm{test}}} \frac{\beta^{\mathrm{LB}}(\mu)}{\beta(\mu)} = 0.506$, $\mathrm{avg}_{\mu\in\Xi_{\mathrm{test}}} \frac{\beta^{\mathrm{LB}}(\mu)}{\beta(\mu)} = 0.7307$, and (b) $\beta^{\mathrm{LB}}_{\mathrm{SCM}^2}(\mu)/\beta(\mu)$; $\min_{\mu\in\Xi_{\mathrm{test}}} \frac{\beta^{\mathrm{LB}}_{\mathrm{SCM}^2}(\mu)}{\beta(\mu)} = 0.572$, $\mathrm{avg}_{\mu\in\Xi_{\mathrm{test}}} \frac{\beta^{\mathrm{LB}}_{\mathrm{SCM}^2}(\mu)}{\beta(\mu)} = 0.865$.

problems, and problems with a high-dimensional parameter space. We hope to report on this in future work.

Acknowledgements

We thank Professor Yvon Maday of University Paris VI and Professor G.R. Liu of National University of Singapore for helpful discussions. This work was supported by AFOSR grant number FA 9550-07-1-0425.

References

[1] B. O. Almroth, P. Stern, and F. A. Brogan. Automatic choice of global shape functions in structural analysis. *AIAA Journal*, 16:525–528, May 1978.

[2] Y. Chen, J.S. Hesthaven, Y. Maday, and J. Rodriguez. A monotonic evaluation of lower bounds for inf-sup stability constants in the frame of reduced basis methods. *C.R. Acad. Sci. Paris, Series I*, 346:1295–1300, 2009.

[3] Y. Chen, J.S. Hesthaven, Y. Maday and J. Rodriguez. Certified reduced basis methods and output bounds for the harmonic Maxwell's equations. *Siam J. Sci. Comput.*, revision submitted.

[4] S. Deparis, Reduced basis error bound computation of parameter-dependent Navier-Stokes equations by the natural–norm approach, SIAM J. Numer. Anal., 46(4), 2039–2067, 2008.

[5] J. P. Fink and W. C. Rheinboldt. On the error behavior of the reduced basis technique for nonlinear finite element approximations. *Z. Angew. Math. Mech.*, 63:21–28, 1983.

[6] D. B. P. Huynh, N. C. Nguyen, G. Rozza, A. T. Patera, 2007-09, Documentation for rbMIT Software: I. Reduced Basis (RB) for dummies. `http://augustine.mit.edu/methodology/methodology_rbMIT_System.htm` ©MIT, Tech. Lic. Office 12600, Cambridge, MA, US.

[7] D. B. P. Huynh, G. Rozza, S. Sen, and A. T. Patera. A successive constraint linear optimization method for lower bounds of parametric coercivity and inf-sup stability constants. *CR Acad Sci Paris Series I*, 345:473–478, 2007.

[8] E. Isaacson, H. B. Keller, Computation of Eigenvalues and Eigenvectors, Analysis of Numerical Methods. Dover Publications, New York, 1994.

[9] C. R. Johnson, A Gershgorin-type lower bound for the smallest singular value, Linear Algebra and Appl, 112 (1989) 1–7.

[10] D. J. Knezevic, A. T. Patera, A certified reduced basis method for the Fokker–Planck equation of dilute polymeric fluids: FENE dumbbells in extensional flow. *Submitted to SIAM J. Sci. Comput.*, May 2009.

[11] N. C. Nguyen, K. Veroy and A. T. Patera. Certified real-time solution of parametrized partial differential equations. *Handbook of Materials Modeling*, (ed. Yip S) Springer 1523–1558, 2005.

[12] A. K. Noor and J. M. Peters. Reduced basis technique for nonlinear analysis of structures. *AIAA Journal*, 18(4):455–462, April 1980.

[13] B. N. Parlett, The Symmetric Eigenvalue Problem, Society for Industrial and Applied Mathematics, Philadelphia, 1998.

[14] T. A. Porsching. Estimation of the error in the reduced basis method solution of nonlinear equations. *Mathematics of Computation*, 45(172):487–496, October 1985.

[15] C. Prud'homme, D. Rovas, K. Veroy, Y. Maday, A. T. Patera, and G. Turinici. Reliable real-time solution of parametrized partial differential equations: Reduced-basis output bound methods. *Journal of Fluids Engineering*, 124(1):70–80, March 2002.

[16] A. Quarteroni and A. Valli Numerical Approximation of Partial Differential Equations. Springer, 2nd edn., 1997.

[17] G. Rozza, D.B.P. Huynh, and A.T. Patera. Reduced basis approximation and a posteriori error estimation for affinely parametrized elliptic coercive partial differential equations application to transport and continuum mechanics. *Archives of Computational Methods in Engineering*, 15:229–275, 2008.

[18] S. Sen, K. Veroy, D. B. P. Huynh, S. Deparis, N. C. Nguyen, and A. T. Patera. Natural norm *a posteriori* error estimators for reduced basis approximations. *Journal of Computational Physics*, 217(1):36–62, 2006.